Can global models ignore the chemical composition of aerosols?

E. L. Roesler[1] and J. E. Penner[1]

[1]   The number of cloud droplets formed from a population of aerosols depends on the aerosol number concentration, N_A, the size distribution, and the chemical composition. The cloud albedo effect occurs when increasing N_A causes increases to the droplet concentration, N_D. We examined the effects of changing aerosol size, composition, and number on N_D within the United States. We found that changing the water-soluble organic carbon (WSOC) fraction from 50% to 0.05% in the fine mode aerosol and from 50% to 95% in the coarse mode aerosol decreased N_D by an average of 34%. Our results show that the changes to the aerosol composition cause over a 20% change to N_D, a magnitude previously estimated to cause a 1 W m^{-2} change in radiative forcing. Given the realistic range of aerosol compositions used here, it is not possible for global models to correctly calculate the cloud albedo effect if composition is ignored. **Citation:** Roesler, E. L., and J. E. Penner (2010), Can global models ignore the chemical composition of aerosols?, *Geophys. Res. Lett.*, *37*, L24809, doi:10.1029/2010GL044282.

1. Introduction

[2] The largest uncertainty in climate change forcing [*Forster et al.*, 2007] is the cloud albedo effect. Global models use empirical relationships based on regional studies or mechanistic activation schemes to calculate N_D [e.g., *Pringle et al.*, 2009]. A focus of current research is to understand which microphysical variables have dominant roles, thereby eliminating the need for global models to keep unnecessary variables. For example, previous studies have shown that aerosol microphysical variables such as size, number, and small concentrations of coarse mode aerosols in a population of fine mode aerosols dominate in the prediction of N_D [*Chen and Penner*, 2005; *Dusek et al.*, 2006; *Feingold et al.*, 1999; *Feingold*, 2003]. Other studies have shown crustal and organic aerosols also influence N_D [*Ervens et al.*, 2005; *Kelly et al.*, 2007; *Nenes et al.*, 2002]. Based on these studies, we changed the microphysical variables in a warm microphysics model to identify which variables changed N_D by 10–20%. These limits of change in N_D were chosen because a decrease in radiative forcing of -1 W m^{-2} has been estimated if N_D is increased by 20% [*Facchini et al.*, 1999].

2. Model Description and Input Parameters

[3] We used the Parcel Undergoing Thermodynamic Transitions (PUTT), a warm microphysics model [*Seidl*, 1989]. The initial relative humidity of the parcel was 98% and was lifted adiabatically 300 meters from an initial starting pressure of 900 mbars at a speed, w, of 10, 20, 50, 150, or 300 cm s^{-1}. The size distribution of the aerosols was modeled as the sum of two lognormal functions each discretized into ninety bins.

[4] The Interagency Monitoring of Protected Visual Environments (IMPROVE) network dataset was used to create the aerosol composition (IMPROVE, IMPROVE Archived Data, 2007, available at http://vista.cira.colostate.edu/improve). The dataset includes 187 sites within the continental United States, Alaska, Hawaii, and the U.S. Virgin Islands (see Figure 1a). Particulate matter monitoring has occurred at some but not all sites from 1988 to 2004. The data was averaged into four seasons for each of the 28 regions listed by *Malm et al.* [1994].

[5] PUTT also calculates the absorption of nitric acid gas, HNO$_{3(g)}$, into the aerosol particles. The parcel's initial gas-phase nitrate concentrations, 0.01 to 31.3 ppbv, were derived from the model results of *Feng and Penner* [2007] for each region and season. *Feng and Penner* [2007] found the model overpredicted the observations in North America. A constant value of 0.2 ppbv for each region and season, which would have given better agreement with the observations, was used in a sensitivity test.

[6] The predicted values for N_D have different responses to internal and external aerosol mixtures [*McFiggans et al.*, 2006], and small concentrations of large aerosols can greatly affect N_D as well as the formation of precipitation [*Feingold et al.*, 1999]. The IMPROVE dataset does not provide the coarse mode PM$_{10.0}$ aerosol composition, size distribution parameters, or the mixing state of the fine and coarse mode aerosols. Measurements taken near the Owens (dry) Lake, a saline playa with large and frequent dust storms in the spring and fall [*Labban et al.*, 2004], were used to constrain the coarse mode aerosol parameters. The composition of the fine mode was similar to the coarse mode aerosols [*Labban et al.*, 2004]. The fine mode composition in the IMPROVE regions affected by Owens (dry) Lake dust storms was also similar to the fine mode measurements by *Labban et al.* [2004]. It was assumed that the fine and coarse mode compositions were equal for these regions in PUTT. Relevant measurements were not available for the composition of the coarse mode for the remainder of the regions. All regions were then assumed to have the same fine and coarse mode composition. This assumption was tested with sensitivity tests where differing fine and coarse mode compositions were used. We assumed the IMPROVE data, when averaged, was an aged background aerosol composition, so external mixtures were not used.

[7] A large component of the fine aerosol mass in the IMPROVE network is organic carbon (OC), but the fraction of OC that is water-soluble is not given [*Malm et al.*, 1994, 2004]. We assumed 50% of the OC was WSOC. Measurements have found WSOC fractions in this range [*Lowenthal*

[1]Department of Atmospheric, Oceanic, and Space Sciences, University of Michigan, Ann Arbor, Michigan, USA.
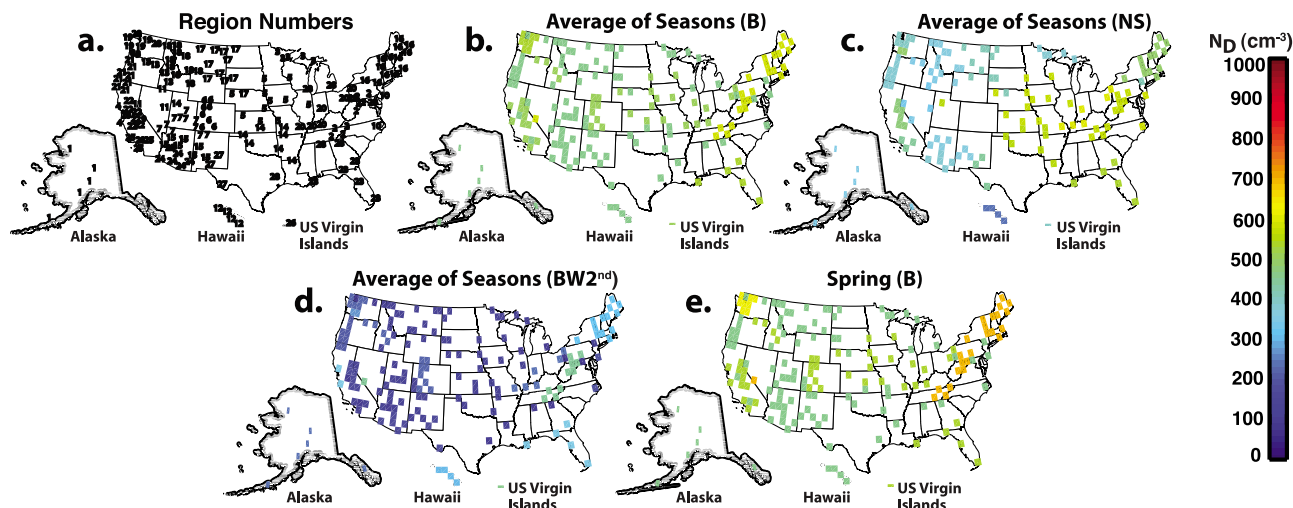
Figure 1. (a) The 28 regions created from the 187 IMPROVE network locations. (b) Droplet concentration, N_D (cm^{-3}) for $w = 20$ cm s^{-1} average of seasons for case B. (c) Same as Figure 1b but with case NS. (d) Same as Figure 1b but with case BW2nd. (e) Same as Figure 1b but with the spring season compositions.

et al., 2009; *Pio et al.*, 2007]. Sensitivity tests also examine this assumption.

[8] Values for the van't Hoff factor, molecular weight, density, charge, and soluble fraction of OC were needed for the WSOC. *Ervens et al.* [2005] suggested that a van't Hoff factor of one produced the lowest error in predicting N_D, and *Mircea et al.* [2005] showed that the average predicted N_D was 20% smaller than the measured N_D when the organics were assumed undissociated. *Ervens et al.* [2005] also found that high molecular weight species (M > 400 g mol^{-1}) influence droplet concentrations. For simplicity, we assumed the WSOC had a molecular weight of 50 grams mol^{-1}, a van't Hoff factor of one, a density of 2.0 grams cm^{-3}, and carried no charge.

[9] Two parameterizations of surface tension, σ_T, were compared in this study. *Mircea et al.*'s [2005] parameterization and treating σ_T as the sum of the multi-component aqueous solution [e.g., *Topping et al.*, 2007]. PUTT's treatment of σ_T had previously accounted for only the inorganic aerosol components [*Seidl*, 1989]. We included values of surface tension as a function of WSOC taken under a variety of atmospheric conditions (i.e., polluted continental, remote continental, biomass burning conditions, and wet-season) [*Facchini et al.*, 1999, 2000; *Mircea et al.*, 2005].

3. Description of Sensitivity Cases

[10] Table 1 lists the base cases and test cases we considered. B, N, and NS are the base cases to which other cases are compared. The base cases use the aerosol compositions created from IMPROVE and are different in N_A and σ_g. Any cases not marked with an S use a geometric standard deviation and mode radius fit to the size distribution of *Dusek et al.* [2006] in the fine mode ($\sigma_{g,f} = 1.5$) and of *Niemeyer et al.* [1999] for the coarse mode ($\sigma_{g,c} = 1.5$). Cases marked with an S use $\sigma_{g,f} = 2.0$ and $\sigma_{g,c} = 3.5$. For cases 1, 3–12, and 21, N_A was calculated for each region from the measured mass concentration in IMPROVE. For cases 2 and 13–20, all regions have a fine and coarse mode

number concentration of $N_{A,f} = 1000$ cm^{-3} and $N_{A,c} = 0.75$ cm^{-3}, respectively, based on typical continental N_A values [*Seinfeld and Pandis*, 2006]. For all cases, the fine mode and coarse mode radii are 0.03 μm and 0.3 μm, respectively.

[11] Cases marked with a G assume [HNO$_3$]$_{(g)}$ = 0.2 ppbv in every region, otherwise results from *Feng and Penner* [2007] were used. Cases marked with a C used a simplified composition of 6% H$^+$, 48% SO$_4^-$, 20% WSOC, and 26% insoluble components in every region, derived from a correlation of the droplet numbers with each component of the composition over all regions and vertical velocities in cases B, BS, and BG. Surface tension was calculated using *Mircea et al.*'s [2005] parameterization, but cases marked st calculate σ_T as the sum of the multi-component aqueous solution. Cases marked ln1 used only the fine mode mass and concentration to explore how neglecting the course mode mass would affect N_D. Cases marked H assumed that a gas-aerosol nitric acid equilibrium is not achieved prior to updraft. For all simulations, the accommodation coefficient for [HNO$_3$]$_{(g)}$ was equal to 0.05 [*Xue et al.*, 2005]. There is uncertainty in the value of the water vapor accommodation coefficient, α [*McFiggans et al.*, 2006]. Cases labeled A set α to 1.0 instead of 0.1. Cases labeled Win assume 50% and 0.05% of the OC in the fine and coarse modes, respectively, is WSOC. Cases labeled W2nd assume 0.05% and 95% of the OC in the fine and coarse modes, respectively, is WSOC. Cases Win and W2nd test ranges of measured WSOC fractions [*Lowenthal et al.*, 2009; *Pio et al.*, 2007].

4. Case and Regional Comparisons of N_D

[12] Table 1 lists the average difference between each test case and base case normalized by the mean of the base case. Mean droplet number increases with vertical velocity. The largest differences in absolute percentage values for base case B is that with test cases N and BW2nd. The largest differences in absolute percentage values for base case NS is that with test cases N and NSW2nd. An average increase in N_A in test case N creates more droplets than in base cases B and NS. In cases BW2nd and NSW2nd, the amount of

Table 1. Base Cases N, NS, and B and Descriptions of Each Test Case[a]

Description of Changed Microphysical Variable of Test Case From Base Case[b]	Mean of $\frac{(N_{Di,test} - N_{Di,base})}{\text{Mean of } (N_{D,base})} \times 100\%$; and Mean of $N_{D,test}$ in cm^{-3}				
	10 cm/s	20 cm/s	50 cm/s	150 cm/s	300 cm/s
Case N: N_A Calculated Regionally From IMPROVE					
1. Changing size distribution to $\sigma_{g,f}$ = 2.0 and $\sigma_{g,c}$ = 3.5 **NS**	−33.9%, 250	−43.3%, 438	−53.2%, 850	−64.7%, 1588	−68.8%, 2047
2. Changing to N_A constant in every region, $N_{A,f}$ = 1000 cm^{-3}, $N_{A,c}$ = 0.75 cm^{-3} **B**	−27.8%, 273	−36.7%, 495	−53.7%, 841	−77.2%, −991	−84.8%, 997
3. Changing to constant nitric acid concentration of [HNO$_3$]$_{(g)}$ = 0.2 ppbv **NG**	−2.7%, 369	−2.7%, 762	−3.1%, 1760	−1.5%, 4283	−0.5%, 6519
4. Changing to constant composition of 6% H$^+$, 48% SO$_4^-$, 20% WSOC, 26% Insol. **NC**	11.9%, 421	7.9%, 808	7.8%, 1845	4%, 4128	4%, 6409
Case NS: N_A Calculated Regionally From IMPROVE With $\sigma_{g,f}$ = 2.0, $\sigma_{g,c}$ = 3.5					
5. Less WSOC (0.05%) in fine mode and more WSOC (95%) in coarse mode **NSW2nd**	−29.8%, 188	−31.7%, 317	−36.4%, 621	−37.7%, 1207	−35.1%, 1748
6. Changing accommodation coefficient to 1.0 from 0.1 **NSA**	−4.9%, 238	−7.5%, 405	−10.2%, 764	−9.3%, 1441	−7.6%, 1892
7. Not calculating surface tension from WSOC **NSst**	−1.8%, 246	−3%, 425	−3%, 825	−1.8%, 1560	−1.1%, 2025
8. Less WSOC (0.05%) in coarse mode **NSWin**	0.8%, 253	1.1%, 434	t 0.7%, 856	0.1%, 1590	0.2%, 2051
9. Changing to using only the fine mode **NSln1**	0.8%, 253	1%, 434	0.7%, 856	0.2%, 1590	0.7%, 2054
10. Changing nitric acid equilibrium prior to uplift **NSH**	2.2%, 255	3.8%, 446	4.3%, 887	3.8%, 1649	2.4%, 2097
11. Changing to constant composition of 6% H$^+$, 48% SO$_4^-$, 20% WSOC, 26% Insol. **NSC**	4.2%, 233	3.8%, 402	1%, 788	1.1%, 1552	0.4%, 2054
12. Changing size distribution to $\sigma_{g,f}$ = 1.5 and $\sigma_{g,c}$ = 1.5 **N**	51.3%, 379	76.3%, 783	114%, 1817	183%, 4349	220%, 6551
Case B: N_A Constant Regionally, $N_{A,f}$ = 1000 cm^{-3}, $N_{A,c}$ = 0.75 cm^{-3}					
13. Less WSOC (0.05%) in fine mode and more WSOC (95%) in coarse mode **BW2nd**	−47.2%, 144	−53.5%, 230	−55.1%, 377	−39.8%, 597	−24.9%, 749
14. Changing size distribution to $\sigma_{g,f}$ = 2.0 and $\sigma_{g,c}$ = 3.5 **BS**	−29.9%, 191	−30.8%, 342	−27%, 614	−10.3%, 889	−5.5%, 943
15. Changing to constant nitric acid concentration of [HNO$_3$]$_{(g)}$ = 0.2 ppbv **BG**	−10.4%, 244	−6.7%, 462	−3.2%, 814	−0.3%, 989	−0%, 997
16. Changing accommodation coefficient to 1.0 from 0.1 **BA**	−4.4%, 261	−8.4%, 453	−6.8%, 784	−1.5%, 976	−0.1%, 996
17. Changing to constant composition of 6% H$^+$, 48% SO$_4^-$, 20% WSOC, 26% Insol. **BC**	2.9%, 281	−1.4%, 488	0.2%, 842	0.5%, 996	0%, 997
18. Changing nitric acid equilibrium prior to uplift **BH**	5.6%, 286	2.6%, 504	2.2%, 860	0.1%, 992	0%, 997
19. Less WSOC (0.05%) in coarse mode **BWin**	8.5%, 294	0.4%, 497	0.9%, 849	0.1%, 992	0%, 997
20. Changing to using only the fine mode **Bln1**	9.7%, 297	0.6%, 498	1%, 850	0%, 991	−0.1%, 997
21. Calculating aerosol number concentration based on IMPROVE mass concentration **N**	38.4%, 379	58%, 783	116%, 1817	339%, 4349	557%, 6551

[a]The five columns from the right list the mean of the difference of N_D in the ith region of the test case from the base case normalized by mean of N_D for all regions in the base case. The mean N_D in cm^{-3} of all regions for each test case is listed after the percentage.

[b]Test case acronym is listed in bold.

soluble mass was decreased in the fine mode and increased in the coarse mode causing the larger, but fewer, more soluble aerosols to form droplets at the expense of the smaller, more numerous, less soluble fine mode aerosols. The third largest difference for N_D for base case B is with test case BS. This is due to the increased width of the size distribution and higher concentration of large-radii aerosols forming droplets at the expense of the small-radii aerosols. The remainder of the sensitivity tests did not have average differences greater than 20% for N_D between the base cases and test cases.

[13] The inter-regional variation (standard deviation divided by the mean N_D) shows how the changes in composition between regions or changes in the microphysical variables affect N_D. A high inter-regional variation value of N_D for a case implies an empirical relationship of N_D based on a region's value would not be accurate if applied to other regions. Figures 1b–1e show N_D (cm^{-3}) in every region for a subset of the test cases from Table 1. Changes in composition between regions cause an inter-regional variation in N_D of 8% when all the seasons are averaged (Figure 1b), and a 15% variation of N_D in the spring (Figure 1e). The mean N_D is increased by 6% to 534 cm^{-3} in spring compared to the annual average mostly due to a factor-of-two average

increase in [HNO$_3$]$_{(g)}$. The N_D in spring is increased by 20% along the eastern U.S. in regions 2 and 16 primarily due to an average increase in [HNO$_3$]$_{(g)}$ from 13 to 26 ppbv. The N_D in regions 8, 9, and 19 also increased by 15% due to the increase in [HNO$_3$]$_{(g)}$ from 7 to 14 ppbv. Changes to the composition caused changes to N_D within and between regions by 10–20%.

[14] The annual average of N_D for base case NS, shown in Figure 1c, has the same aerosol composition as the annual average of base case B (Figure 1b), and N_A is also unique in every region which causes an inter-regional variation of 48%. The average N_D decreased by 12% compared to case B due to an average decrease in N_A in case NS. Figure 1d shows the BW2nd case which has the largest inter-regional variation of 60%. From Table 1, case BS has the third largest average difference in N_D from base case B but has a negligible inter-regional variation (not shown in Figure 1). This is due to the increased width of the size distribution and higher concentration of large-radii aerosols forming droplets at the expense of the small-radii aerosols.

5. Changes to N_D for Different S_{max}

[15] Figure 2 shows the computed N_D at the maximum supersaturation, S_{max}, for test cases 5–12 against base case
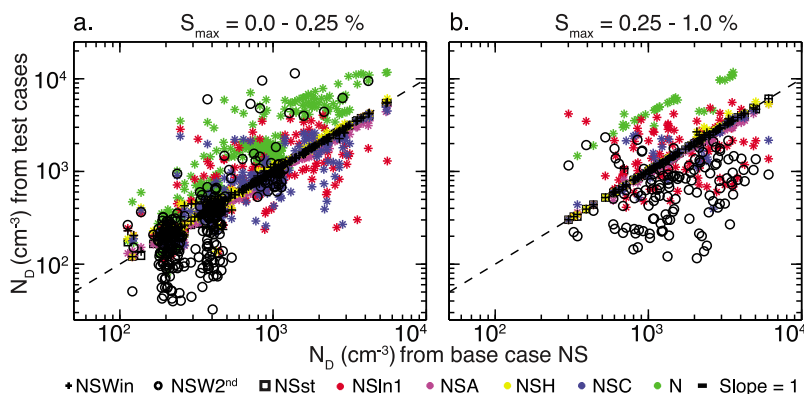
Figure 2. Scatter plots of droplet concentration, N_D, of all seasons and regions at the parcel's S_{max} for different test cases compared to the base case NS in two maximum supersaturation (S_{max}) ranges. (a) S_{max} range, 0.0–0.25%. Cases NSW2nd, NSln1, NSC, N, and NSA have correlations of 0.69, 0.72, 0.87, 0.88, and 1.0 with slopes of 2.34, 0.70, 0.79, 2.42, and 0.85, respectively. (b) S_{max} range, 0.25–1.0%. Cases NSW2nd, NSln1, NSC, N, and NSA and have correlations of 0.23, 0.28, 0.83, 0.93, and 1.0 with slopes of 0.12, 0.28, 0.73, 2.59, and 0.85, respectively. In both Figures 2a and 2b, cases NSH, NSst, and NSWin have correlations of ~1.0 with slopes of ~1.0.

NS separated into two S_{max} ranges. This was done to examine whether a parameterization of the base case that is a function of S_{max} and N_A could be used. Slopes of best-fit lines and correlation coefficients were calculated and are reported in the caption. A test case that has a low correlation with the base case NS suggests an empirical relationship formed from the base case would not correctly predict N_D.

[16] For both the low and high ranges of S_{max}, cases NSH, NSst, and NSWin have slopes and correlations of ~1.0. This indicates that a parameterization would not need to include changes in the gas-aerosol equilibrium of nitric acid prior to updraft, the parameterization of surface tension, or a small concentration of coarse-mode aerosols with less soluble mass. In both the low and high ranges of S_{max}, cases NSC, N, and NSA all have correlation coefficients greater than 0.83 with slopes that range from 0.73 to 2.60. If a parameterization that is based on simplified composition or inaccurate N_A and σ_g is applied, then the calculated average N_D and cloud albedo effect will also be inaccurate. Case NSln1 shows a correlation and slope of ~0.70 at low S_{max}, but a correlation and slope of 0.28 at high S_{max}. For the low and high ranges of S_{max}, NSW2nd has correlations and slopes much different from 1.0. Thus an empirical relationship that is based on aerosol parameters similar to case NS could not correctly calculate N_D if applied to other regions that had a different number of modes or amount of soluble material.

6. Conclusions

[17] Measurements of aerosols in Europe have shown that the aerosol size distribution mostly determines the aerosol's ability to become a cloud droplet [*Dusek et al.*, 2006]. In this study, it was found that the aerosol size distribution and composition cannot be ignored by global models when calculating the N_D for the cloud albedo, which is based aerosol compositions measured in the United States from 1988 to 2004. These results are based on assumptions regarding the size-resolved and physicochemical properties of WSOC. Changing these assumptions would affect N_D, and further sensitivity studies could identify which WSOC properties were most important for modeling. A global model using an empirical relationship based on regional measurements could over- or under-predict N_D when applied to other regions depending on differences in composition, the number of log-normal modes, N_A, and σ_g. Regional and seasonal differences in trace gas concentrations, organic, inorganic, and insoluble aerosol compositions cause high variability in N_D, suggesting a more thorough treatment and not a simplification of aerosol composition is needed for an accurate prediction of N_D.

References

Chen, Y., and J. E. Penner (2005), Uncertainty analysis for estimates of the first indirect aerosol effect, *Atmos. Chem. Phys.*, *5*, 2935–2948.

Dusek, U., et al. (2006), Size matters more than chemistry for cloud-nucleating ability of aerosol particles, *Science*, *312*(5778), 1375–1378.

Ervens, B., G. Feingold, and S. M. Kreidenweis (2005), Influence of water-soluble organic carbon on cloud drop number concentration, *J. Geophys. Res.*, *110*, D18211, doi:10.1029/2004JD005634.

Facchini, M. C., M. Mircea, S. Fuzzi, and R. J. Charlson (1999), Cloud albedo enhancement by surface-active organic solutes in growing droplets, *Nature*, *401*(6750), 257–259.

Facchini, M. C., S. Decesari, M. Mircea, S. Fuzzi, and G. Loglio (2000), Surface tension of atmospheric wet aerosol and cloud/fog droplets in relation to their organic carbon content and chemical composition, *Atmos. Environ.*, *34*(28), 4853–4857.

Feingold, G. (2003), Modeling of the first indirect effect: Analysis of measurement requirements, *Geophys. Res. Lett.*, *30*(19), 1997, doi:10.1029/2003GL017967.

Feingold, G., W. R. Cotton, S. M. Kreidenweis, and J. T. Davis (1999), The impact of giant cloud condensation nuclei on drizzle formation in stratocumulus: Implications for cloud radiative properties, *J. Atmos. Sci.*, *56*(24), 4100–4117.

Feng, Y. and J. E. Penner (2007), Global modeling of nitrate and ammonium: Interaction of aerosols and tropospheric chemistry, *J. Geophys. Res.*, *112*, D01304, doi:10.1029/2005JD006404.

Forster, P., et al. (2007), Changes in atmospheric constituents and in radiative forcing, in *Climate Change 2007: The Physical Science Basis. Contribution of Working Group I to the Fourth Assessment Report of the Intergovernmental Panel on Climate Change*, edited by S. Solomon et al., pp. 129–234, Cambridge Univ. Press, Cambridge, U. K.

Kelly, J. T., C. C. Chuang, and A. S. Wexler (2007), Influence of dust composition on cloud droplet formation, *Atmos. Environ.*, *41*(14), 2904–2916.

Labban, R., J. M. Veranth, J. C. Chow, J. L. P. Engelbrecht, and J. G. Watson (2004), Size and geographical variation in PM1, PM2.5 and PM10: Source profiles from soils in the western United States, *Water Air Soil Pollut.*, *157*(1–4), 13–31.

Lowenthal, D., B. Zielinska, B. Mason, S. Samy, V. Samburova, D. Collins, C. Spencer, N. Taylor, J. Allen, and N. Kumar (2009), Aerosol characterization studies at Great Smoky Mountains National Park, summer 2006, *J. Geophys. Res.*, *114*, D08206, doi:10.1029/2008JD011274.

Malm, W. C., J. F. Sisler, D. Huffman, R. A. Eldred, and T. A. Cahill (1994), Spatial and seasonal trends in particle concentration and optical extinction in the United States, *J. Geophys. Res.*, *99*(D1), 1347–1370.

Malm, W. C., B. A. Schichtel, M. L. Pitchford, L. L. Ashbaugh, and R. A. Eldred (2004), Spatial and monthly trends in speciated fine particle concentration in the United States, *J. Geophys. Res.*, *109*, D03306, doi:10.1029/2003JD003739.

McFiggans, G., et al. (2006), The effect of physical and chemical aerosol properties on warm cloud droplet activation, *Atmos. Chem. Phys.*, *6*, 2593–2649.

Mircea, M., et al. (2005), Importance of the organic aerosol fraction for modeling aerosol hygroscopic growth and activation: A case study in the Amazon Basin, *Atmos. Chem. Phys.*, *5*, 3111–3126.

Nenes, A., R. J. Charlson, M. C. Facchini, M. Kulmala, A. Laaksonen, and J. H. Seinfeld (2002), Can chemical effects on cloud droplet number rival the first indirect effect?, *Geophys. Res. Lett.*, *29*(17), 1848, doi:10.1029/2002GL015295.

Niemeyer, T. C., D. A. Gillette, J. J. Deluisi, Y. J. Kim, W. F. Niemeyer, T. Ley, T. E. Gill, and D. Ono (1999), Optical depth, size distribution and flux of dust from Owens Lake, California, *Earth Surf. Processes Landforms*, *24*(5), 463–479.

Pio, C. A., et al. (2007), Climatology of aerosol composition (organic versus inorganic) at nonurban sites on a west-east transect across Europe, *J. Geophys. Res.*, *112*, D23S02, doi:10.1029/2006JD008038.

Pringle, K. J., K. S. Carslaw, D. V. Spracklen, G. M. Mann, and M. P. Chipperfield (2009), The relationship between aerosol and cloud drop number concentrations in a global aerosol microphysics model, *Atmos. Chem. Phys.*, *9*(12), 4131–4144.

Seidl, W. (1989), Ionic concentrations and initial S(IV)-oxidation rates in droplets during the condensational stage of cloud, *Tellus, Ser. B*, *41*, 32–50.

Seinfeld, J. H., and S. N. Pandis (2006), *Atmospheric Chemistry and Physics: From Air Pollution to Climate Change*, 2nd ed., J. Wiley, Hoboken, N. J.

Topping, D. O., G. B. McFiggans, G. Kiss, Z. Varga, M. C. Facchini, S. Decesari, and M. Mircea (2007), Surface tensions of multi-component mixed inorganic/organic aqueous systems of atmospheric significance: Measurements, model predictions and importance for cloud activation predictions, *Atmos. Chem. Phys.*, *7*(9), 2371–2398.

Xue, H. W., A. M. Moyle, N. Magee, J. Y. Harrington, and D. Lamb (2005), Experimental studies of droplet evaporation kinetics: Validation of models for binary and ternary aqueous solutions, *J. Atmos. Sci.*, *62*(12), 4310–4326.

E. L. Roesler and J. E. Penner, Department of Atmospheric, Oceanic, and Space Sciences, University of Michigan, Space Research Building, 2455 Hayward St., Ann Arbor, MI 48109-2143, USA. (eroesler@umich.edu)